

Design of automatic vision-based inspection system for solder joint segmentation

N.S.S. Mar*, **C. Fookes**, **P.K.D.V. Yarlagadda**

School of Engineering Systems,
Queensland University of Technology,
George Street 2, Brisbane QLD 4001, Australia

* Corresponding author: E-mail address: marn@qut.edu.au

Received 10.02.2009; published in revised form 01.06.2009

Analysis and modelling

ABSTRACT

Purpose: Computer vision has been widely used in the inspection of electronic components. This paper proposes a computer vision system for the automatic detection, localisation, and segmentation of solder joints on Printed Circuit Boards (PCBs) under different illumination conditions.

Design/methodology/approach: An illumination normalization approach is applied to an image, which can effectively and efficiently eliminate the effect of uneven illumination while keeping the properties of the processed image the same as in the corresponding image under normal lighting conditions. Consequently special lighting and instrumental setup can be reduced in order to detect solder joints. These normalised images are insensitive to illumination variations and are used for the subsequent solder joint detection stages. In the segmentation approach, the PCB image is transformed from an RGB color space to a YIQ color space for the effective detection of solder joints from the background.

Findings: The segmentation results show that the proposed approach improves the performance significantly for images under varying illumination conditions.

Research limitations/implications: This paper proposes a front-end system for the automatic detection, localisation, and segmentation of solder joint defects. Further research is required to complete the full system including the classification of solder joint defects.

Practical implications: The methodology presented in this paper can be an effective method to reduce cost and improve quality in production of PCBs in the manufacturing industry.

Originality/value: This research proposes the automatic location, identification and segmentation of solder joints under different illumination conditions.

Keywords: Automatic PCB inspection; Segmentation of solder joints; Illumination normalization; Computer vision

Reference to this paper should be given in the following way:

N.S.S. Mar, C. Fookes, P.K.D.V. Yarlagadda, Design of automatic vision-based inspection system for solder joint segmentation, Journal of Achievements in Materials and Manufacturing Engineering 34/2 (2009) 145-151.

1. Introduction

Assembly of Printed Circuit Boards (PCBs) using Surface Mount Technology (SMT) has been widely used in the electronic industry recently [1]. As a result, the electronic components rely on the solder joint to provide the electrical connection to the PCBs; therefore, the quality of the solder joint can be critical to the quality of the electronic components [2]. Automatic Optical Inspection (AOI) of solder joints has been a critical issue for quality control in PCB assembly as AOI has the enormous potential of completely automating human visual inspection procedures [3, 4]. The aim of these inspection procedures is to detect and locate any potential solder joints defects which will impede or break down the functions of the final PCB products. Common solder joint defects which are of concern include: no solder, opens, shorts, and bridges [5, 26, 27].

Automated solder joint inspection requires the extraction of information from the solder joint surface [6]. However, the specularly of the solder joint surface causes difficulties in the automated extraction of relevant information. Specular reflections of the solder joint surface may appear or disappear with small changes in viewing direction. A specular surface is illuminated at a distance by a point light source which prevents ideal smooth shading that matches its shape for the effective classification of solder joints. Furthermore, the shape of the solder joints tend to vary greatly with soldering conditions including the amount of solder paste and heating level applied during the soldering process. So the variety of the solder joint shapes is also a barrier to the development of an automatic solder joint inspection system. Furthermore, the variety of components on the board and the sophisticated layout of the board introduce more complexity for solder joint inspection which makes the development of automated pattern recognition systems for this purpose a non-trivial task [5].

In this study, a computer vision system is proposed for the automatic detection, localisation, and segmentation of solder joints on PCBs under different illumination conditions. This is referred to as the "front-end" inspection system. The back-end involves the classification of the solder joints which is not addressed in this work. The front-end inspection system includes illumination normalization which is applied to an image to effectively and efficiently eliminate the effect of uneven illumination while keeping the properties of the processed image the same as in the corresponding image under normal lighting condition. Consequently special lighting and instrumental setup can be reduced in order to detect solder joints. A method of using an unloaded PCB which is on the conveyor line is also proposed to identify the positions of solder joints. The process consists of solder joint location identification and automated segmentation of solder joints.

The outline of this paper is as follows. Section 2 will provide an overview of existing inspection techniques in the field. Section 3 will present the proposed automatic "front-end" inspection system including the detection, localisation, and segmentation of solder joint stages. Section 4 will provide some experimental results on real PCB images. Section 5 will conclude the paper.

2. Literature review and current status

The initial application of machine vision for solder joint inspection was concentrated on capturing solder joints under

uniformly diffuse lighting [7]. Besl and Jain used diffusive light to avoid the generation of saturated images caused by specular reflections of the solder joint; however, the results are discouraging partly due to their sensitivity to illumination conditions [8]. A structured high-light approach is also proposed for illumination and imaging of specular surfaces which yields three-dimensional shape information. Features of solder joints are extracted from high-contrast 3D images with a significantly overhead required in computation [9]. The Extended Gaussian Image (EGI) was used for solder joint inspection in which a considerable number of point light sources highlighted the solder joints [10, 11]. The EGI requires too much time in image scanning and image processing hence the use of multiple tiered ring light was subsequently proposed.

Different types of illumination techniques have been used for solder joints inspection system [12]. A circular, tiered illumination system of three colored lamps (red, green, blue) is used to extract information for the solder joint inspection [12-16]. The solder joints are represented as red, green and blue color patterns according to their surface slopes and closely related to their 3D shapes. By examining the 3D features, the solder joint defects could be determined.

Hong provides an efficient solution for solder joint inspection by using structured lighting [1]. An array of LEDs is used as a structured source for detecting solder joint defects. The LED array is placed on the lighting system to project the light source from a different position onto the solder joint surface. Laser inspection can also be used to measure 3D surfaces of solder joints directly but it has a low inspection speed and high cost [3].

Much of the research reported in the literature requires special lighting sources or setups because of the variety of the solder joint shapes. Further research is required to address the development of robust and fully automated inspection systems which can operate in less constrained lighting environments to reduce the cost of and improve the utility of this technology. This requires further advances to be made in the front-end of inspection systems to robustly detect, locate and segment all solder joints from PCBs under any given condition.

3. Research methodology for automated front-end inspection system

This section will outline the four stages involved in the front-end inspection system proposed here. This includes a Hough Transform, Normalization illumination, Color transformation and Allocation of solder joints.

3.1. Hough transform

This approach used the Hough Transform technique to allocate the PCB so that the PCB does not need to be placed onto a precision X-Y table. In this way the PCB can be located on an automatic conveyor line, without interrupting the line production. This algorithm also helps to improve accuracy of the solder joint segmentation.

The Hough Transform method has been recognized as one of the most popular method to extract parameterized lines from an

image [17]. The transform maps a line in the image space (x,y) into a point in the Hough Transform parameter space. For straight line detection, the equation of a line can be expressed as

$$\rho = x \cos(\theta) + y \sin(\theta) \quad (1)$$

where θ and ρ are respectively the orientation of the line and the distance to the origin.

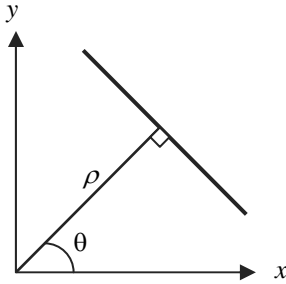


Fig. 1. Parametric description of a straight line

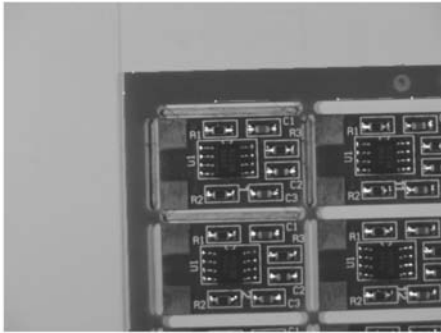


Fig. 2. Acquired image



Fig. 3. Result of Hough Transform

The range of angle θ is $\pm 90^\circ$, measured with respect to the x-axis [18]. Thus with reference to Figure 1, a horizontal line has $\theta = 0^\circ$ with ρ being equal to the positive x-intercept. Similarly, a vertical line has $\theta = 90^\circ$, with ρ being equal to the positive y-intercept, or $\theta = -90^\circ$, with ρ being equal to the negative y-

intercept. With the references from θ and ρ , PCB can be allocated automatically. Figure 2 and 3 show the image before and after applying the Hough transform technique.

3.2. Normalization illumination

Since solder joints are invariant to illumination variation, it results in a challenge for this research. The same solder joint can appear greatly different under varying lighting conditions. In this approach, images are preprocessed using image processing techniques to normalize the images to appear stable under different lighting conditions. Since illumination variations mainly lie in the low-frequency band, an appropriate number of DCT coefficients are truncated to minimize variations under different lighting conditions [19]. There are four established types of Discrete Cosine Transforms (DCT's), i.e., DCT-I, DCT-II, DCT-III and DCT-IV. The DCT-II is more widely applied in signal coding. The 2D $M \times N$ DCT is defined as [19]:

$$C(u,v) = \alpha(u)\alpha(v) \sum_{x=0}^{M-1} \sum_{y=0}^{N-1} f(x,y) \times \cos\left[\frac{\pi(2x+1)u}{2M}\right] \cos\left[\frac{\pi(2y+1)v}{2N}\right] \quad (2)$$

and the inverse transform is defined as

$$f(x,y) = \sum_{u=0}^{M-1} \sum_{v=0}^{N-1} \alpha(u)\alpha(v) C(u,v) \times \cos\left[\frac{\pi(2x+1)u}{2M}\right] \cos\left[\frac{\pi(2y+1)v}{2N}\right] \quad (3)$$

where

$$\alpha(u) = \begin{cases} \frac{1}{\sqrt{M}}, & u = 0 \\ \sqrt{\frac{2}{M}}, & u = 1, 2, \dots, M-1 \end{cases} \quad (4)$$

$$\alpha(v) = \begin{cases} \frac{1}{\sqrt{N}}, & v = 0 \\ \sqrt{\frac{2}{N}}, & v = 1, 2, \dots, N-1 \end{cases}$$

In the proposed approach, the DCT is performed on the entire image to obtain all frequency components of the image.

Equation (5) is used to get the matrix form of equation (1)

$$T_{i,j} = \begin{cases} \frac{1}{\sqrt{N}} & \text{if } i = 0 \\ \sqrt{\frac{2}{N}} \cos\left[\frac{(2j+1)i}{2N}\right] & \text{if } i > 0 \end{cases} \quad (5)$$

The Discrete Cosine Transform is accomplished by the matrix multiplication as in the equation (6)

$$D = TMT' \quad (6)$$

In the equation (6) matrix of image-pixel values is first multiplied on the left by the DCT matrix T to transform the rows

[20]. The columns are then transformed by multiplying on the right by the transpose of the DCT matrix.

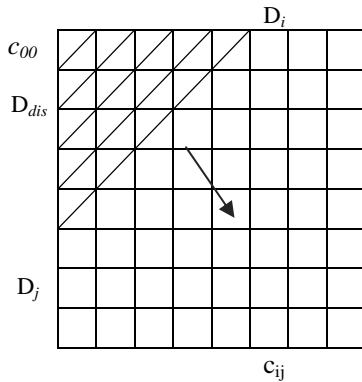


Fig. 4. Manner of discarding DCT coefficients (only the first 8 x 8 coefficients are shown)



Fig. 5. Original image



Fig. 6. Reconstructed image by applying the DCT

This block matrix consists of DCT coefficients, D_{ij} . The top-left coefficient, c_{00} is correlated to the low frequencies of the original image block. As c_{00} is removed, the DCT coefficients correlate to higher and higher frequencies of the image block, where c_{ij} corresponds to the highest frequency. It is important to eliminate the low frequency which is the most sensitive to human eye. The manner of discarding DCT coefficients is shown in Figure 4.

As illustrated in Figures 5 and 6, the original image is improved by applying the DCT.

3.3. Color transformation

It is not easy to separate the solder joints and other background from a PCB image, because there are many lines and markings that have similar values as the solder joint [5]. In this case, the PCB image is transformed from RGB color model to YIQ color model. The advantages of YIQ color model are 1) processing Y component only will differ from unprocessed image in its appearance of brightness and 2) most high frequency components of a color image are in Y. The image is transformed to YIQ, which gives one luminance signal Y and two color signals I&Q. Again, I stands for in-phase, while Q stands for quadrature, referring to the components used in quadrature amplitude modulation [21]. Equation (7) and (8) describe the transformations between the RGB and YIQ color spaces.

$$\begin{bmatrix} Y \\ I \\ Q \end{bmatrix} = \begin{bmatrix} 0.2290 & 0.5870 & 0.1140 \\ 0.5957 & -0.2744 & -0.3213 \\ 0.2115 & -0.5226 & 0.3111 \end{bmatrix} \begin{bmatrix} R \\ G \\ B \end{bmatrix} \quad (7)$$

$$\begin{bmatrix} R \\ G \\ B \end{bmatrix} = \begin{bmatrix} 1 & 0.9563 & 0.6210 \\ 1 & -0.2721 & -0.6740 \\ 1 & -1.1070 & 1.7046 \end{bmatrix} \begin{bmatrix} Y \\ I \\ Q \end{bmatrix} \quad (8)$$

3.4. Allocation of solder joints

Thresholding

After performing the color transformation of an image, a solder joint needs to be extracted from its background by a threshold selection. If the object has a different average gray level from that of its background, it is often difficult to select an appropriate threshold. In this research, a successive iterative process is described to get an optimum threshold [22]. The histogram of an image is initially segmented into two parts using a starting threshold value such as half the maximum dynamic range. Then, the sample data are computed into two classes which are the sample mean of the gray values associated with the foreground pixels and the sample mean of the gray values associated with the background pixels. Then a new threshold value is computed as the average of the above two sample means. The resultant threshold and its upper and lower thresholds are applied to the PCB image. Then the new threshold value is calculated according to the number of components detected. This process is repeated until the numbers of component do not change any more.

Region Filling

Although the solder joint have been detected, closed or opened holes might occur on solder joints after segmentation because of the surface property and shape of solder joints [2].

These holes can be confusing when determining of solder joint location. So those holes need to be mended. Firstly, erosion and dilation of Morphology is applied to enclose an opened hole. If dilation of Morphology is used to enclose a hole, it might change the original shape of the solder joints. In that case, Region Filling is applied to mend these closed holes. Region Filling is based on set dilations, complementation, and intersections [23]. In Figure 7 A denotes a set containing a subset whose elements are 8-connected boundary points of a region.

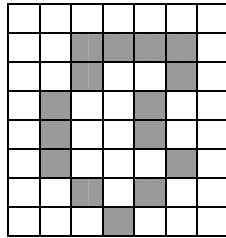


Fig. 7. Set A

Beginning with a point p inside the boundary, the objective is to fill the entire region with 1's. The following equation is used to fill the region with 1's:

$$X_k = (X_{k-1} \oplus B) \cap A^c \quad k = 1, 2, 3, \dots \quad (9)$$

where $X_0 = p$, and B is the symmetric structuring element. The algorithm terminates at iteration step k if $X_k = X_{k-1}$. The set union of X_k and A contains the filled set and its boundary. The result of region filling is shown in Figure 8.

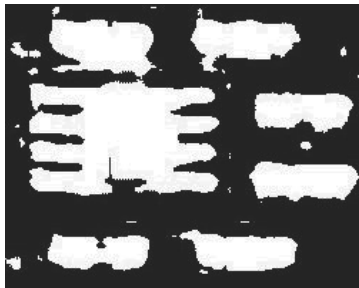


Fig. 8. Result of Region Filling

Segmentation Process

There are two stages in the segmentation process. In the first stage of segmentation, components are extracted from the acquired image and the next step is to extract an image of the solder joint from each component.

In performing the first step of segmentation, the pixels which represent component and background are grouped into meaningful regions [24]. The white pixels correspond to component and black pixels correspond to background. Once an object pixel is found, the entire connected object region is enumerated. Finally, the centroid of the region is calculated as a simple measure of object location. Figure 9 shows after applying the segmentation on the PCB board.

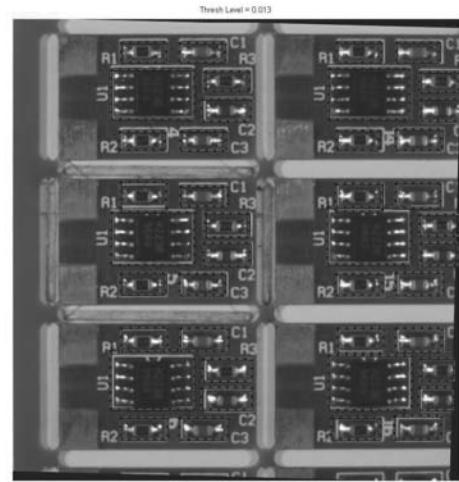


Fig. 9. An example of detected components from database 1

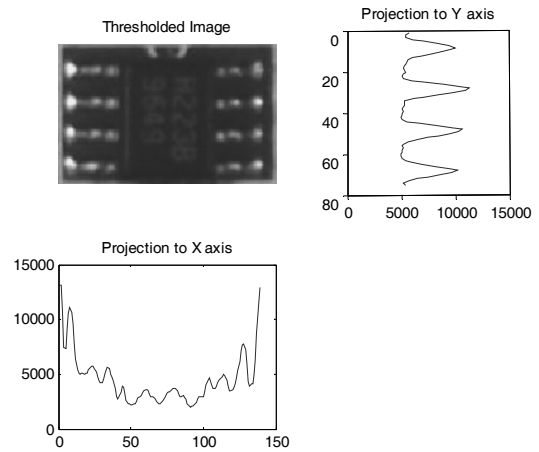


Fig. 10. Image processing of solder joint

For the next step of segmentation, each solder joint can be isolated by projection of image horizontally and vertically. Each lead-pad pair can be isolated by vertical projection and the solder region can be identified by horizontal projection (i.e. Figure 10). Suppose $p \times m$ is a matrix associated with the thresholded image. The equations for the horizontal projection H and the vertical projection V are defined as follows:

$$H = \sum_{i=1}^p \rho_i \quad (10)$$

$$V = \sum_{j=1}^m \gamma_j \quad (11)$$

where ρ_i and γ_j are the i -th row and j -th column of the image.

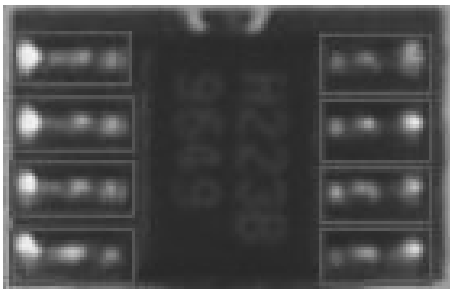


Fig. 11. An example of detected solder joints from database 1



Fig. 12. An example of detected solder joints from database 2

The proposed system is implemented under Matlab 7.4.0287 (R2007a) [25].

4. Results and discussion

Two sets of solder joint databases are used in the experiments. The test images for database 1 were supported from Ahmed Nabil Belbachir (Vienna University of Technology) and those of Database 2 were taken by digital camera under a fluorescent light source. The total of 3840 (database 1) and 621 (database 2) solder joints are used in these experiments. The parameter such as the size of solder joints is approximately defined. Four indices were used to evaluate the segmentation results:

- Hit rate: percentage of correct detected joints
- Miss rate: percentage of undetected joints
- False rate: percentage of incorrect detected joints

Four different types of experiments have been performed on solder joint images. The first experiment is conducted with the combination of two algorithms; normalization illumination and automatic thresholding which gives the best result with a 99.93% success rate. The second experiment is performed for automatic thresholding without illumination normalization. The third and fourth experiments were performed for manual thresholding with and without illumination normalization. The manual threshold value is selected by plotting the resultant thresholding value from automatic thresholding and selecting its mean value. From these experiments, it can be clearly seen that the success rate is very

low for manual thresholding without illumination normalization with a 78.94% success rate. The results of the test stage are summarized in Tables 1 and 2 for database 1 and 2.

Table 1.

The segmentation result for database 1

Condition of experiment	Hit rate (%)	Miss rate (%)	False rate (%)
Automatic thresholding with normalization illumination	99.93	0.07	0
Automatic thresholding without normalization illumination	99.70	0.3	0
Manual thresholding with normalization illumination	97.56	2.23	0.21
Manual thresholding without Normalization illumination	78.94	20.91	0.15

Table 2.

The segmentation result for database 2

Condition of experiment	Hit rate (%)	Miss rate (%)	False rate (%)
Automatic thresholding with normalization illumination	99.83	0.17	0
Automatic thresholding without normalization illumination	99.03	0.64	0.24
Manual thresholding with normalization illumination	96.62	3.38	0
Manual thresholding without normalization illumination	81.64	18.04	0.32

5. Conclusions

In this paper, an automatic segmentation approach for detection of solder joints has been presented. The segmentation approach which is based on the YIQ model is easy to handle and obtains good results. This process requires no special lighting device or setup and can apply a simple thresholding and segmentation algorithm. In general, the same techniques should be applied on other object segmentation such as BGA inspection, solder paste inspection and IC lead inspection etc.

Acknowledgements

Test images were supported by Mr. Ahmed Nabil Belbachir (Vienna University of Technology).

References

- [1] H.H. Lo, M.S. Lu, Printed circuit board inspection using image analysis, *IEEE Transactions on Industry Applications* 35/2 (1999) 426-432.
- [2] Z.S. Lee, R.C. Lo, Application of vision image cooperated with multi-light sources to recognition of solder joints for PCB TAAI, *Artificial Intelligence and Applications* (2002) 425-430.
- [3] Y. Fang-Chung, K. Chung-Hsien, W. Jein-Jong, Y. Ching-Kun, Reconstructing the 3D solder paste surface model using image processing and artificial neural network, *Systems, Man and Cybernetics* 3 (2004) 3051-3056.
- [4] L. Shih-Chieh, C. Chih-Hsien, S. Chia-Hsin, A development of visual inspection system for surface mounted devices on printed circuit board, *Proceedings of the 33rd Annual Conference of the IEEE Industrial Electronics Society (IECON) Taipei, Taiwan, 2007*, 2440-2445
- [5] B. C. Jiang, C.C. Wang, Y.N. Hsu, Machine vision and background remover-based approach for PCB solder joints inspection, *International Journal of Production Research* 45/2 (2007) 451-464.
- [6] J.H. Kim, H.S. Cho, S. Kim, Pattern classification of solder joint images using a correlation neural network, *Engineering Applications of Artificial Intelligence* 9/6 (1996) 655-669.
- [7] S.L. Bartlett, P.J. Besl, C.L. Cole, R. Jain, D. Mukherjee, K.D. Skifstad, Automatic solder joint inspection, *IEEE Transactions on Pattern Analysis and Machine Intelligence* 10/1 (1988) 31-43.
- [8] P.J. Besl, E.J. Delp, R. Jain, Automatic visual solder joint inspection, *IEEE Journal of Robotics and Automation* 1/1 (1985) 42-56.
- [9] A.C. Sanderson, L.E. Weiss, S.K. Nyar, Structured highlight inspection of specular surfaces, *IEEE Transactions on Pattern Analysis and Machine Intelligence* 10/1 (1988) 44-55.
- [10] S.K. Nayar, A.C. Sanderson, L.E. Weiss, D.A. Simon, Specular surface inspection using structured highlight and Gaussian images, *IEEE Transactions on Robotics and Automation* 6/2 (1990) 208-218.
- [11] Y.K. Ryu, H.S. Cho, A neural network approach to Extended Gaussian Image based solder joint inspection, *Mechatronics* 7/2 (1997) 159-184.
- [12] T.H. Kim, T.H. Cho, Y.S. Moon, S.H. Park, Visual inspection system for the classification of solder joints, *Pattern Recognition* 324 (1999) 565-575.
- [13] J.H. Kim, H.S. Cho, Neural network-based inspection of solder joints using a circular illumination, *Image and Vision Computing* 13/6 (1995) 479-490.
- [14] K.W. Ko, H.S. Cho, Solder joints inspection using a neural network and fuzzy rule-based classification method, *IEEE Transactions on Electronics Packaging Manufacturing* 23/2 (2000) 93-103.
- [15] T.S. Yun, K.J. Sim, H.J. Kim, Support vector machine-based inspection of solder joints using circular illumination, *Electronics Letters* 36/11 (2000) 949-951.
- [16] D.W. Capson, S.K. Eng, A tiered-color illumination approach for machine inspection of solder joints, *IEEE Transactions on Pattern Analysis and Machine Intelligence* 10/3 (1988) 387-393.
- [17] R. Fisher, S. Perkins, A. Walker, E. Wolfart, *Hypermedia image processing reference*, Published by J.Wiley & Sons, Ltd. Published by J.Wiley & Sons, Ltd. 1996.
- [18] R.C. Gonzalez, R.E. Woods, S.L. Eddins, *Digital image processing using Matlab*, First ed, Pearson Prentic Hall, 2004.
- [19] W. Chen, M.J. Er, S. Wu, Illumination compensation and normalization for robust face recognition using discrete cosine transform in logarithm domain, *IEEE Transactions on Systems, Man, and Cybernetics-Part B* 36/2 (2006) 458-466.
- [20] C. Ken, G. Peter, Image compression and the discrete cosine transform, 1998, <http://online.redwoods.cc.ca.us/instruct/darnold/laproj/Fall98/PKen/dct.pdf>.
- [21] A.A. Al-Nu'aimi, R. Qahwaji, Digital colored image watermarking using YIQ color format in discrete wavelet transform domain, <http://www.stcex.gotenvot.edu.sa/NR/rdonlyres/A00DB3B0-7993-40A5-BE34-C3293D76637D/0/305.pdf>.
- [22] T.W. Ridler, S. Calvard, Picture thresholding using an iterative selection method, *IEEE Transactions on Systems, Man and Cybernetics* 8/8 (1978) 630-632.
- [23] R.C. Gonzalez, R.E. Woods, *Digital image processing*, Second ed, Pearson Prentic Hall, 2002.
- [24] E. Frew, A. Huster, E. LeMaster, Image thresholding for object detection, 1997.
- [25] MathWorks Inc., *Matlab: The language of technical computing*.
- [26] A. Klimpel, A. Lisiecki, J. Szlek, Welding of girders to insert plates of composite steel-concrete structure of tower in Kuwait, *Archives of Materials Science and Engineering* 28/7 (2007) 433-436.
- [27] S. Wiewiórska, Z. Muskalski, M. Suliga, M. Pełka, The numerical analysis of Hi-temp 095 wire drawing process, *Journal of Achievements in Materials and Manufacturing Engineering* 27/2 (2007) 175-178.